

Band engineering of bilayer graphene by metal atoms: First-principles calculations

D.-H. Oh,^{1,a)} B. G. Shin,¹ and J. R. Ahn^{1,2,b)}

¹BK21 Physics Research Division, Sungkyunkwan University, Cheoncheon-dong 300, Jangan-gu, Suwon, Republic of Korea

²SKKU Advanced Institute of Technology, Sungkyunkwan University, Cheoncheon-dong 300, Jangan-gu, Suwon, Republic of Korea

(Received 19 April 2010; accepted 21 May 2010; published online 11 June 2010)

The continuous change in the electronic band structure of metal-adsorbed bilayer graphene was calculated as a function of metal coverage using first-principles calculations. Instead of modifying the unit cell size as a function of metal coverage, the distance between the metal atoms and bilayer graphene in the same 2×2 unit cell was controlled to change the total charges transferred from the metal atoms to bilayer graphene. The validity of the theoretical method was confirmed by reproducing the continuous change in the electronic band structure of K-adsorbed epitaxial bilayer graphene, as shown by Ohta *et al.* [Science **313**, 951 (2006)]. In addition, the changes in the electronic band structures of undoped, n-type, and p-type bilayer graphene were studied schematically as a function of metal coverage using the theoretical method. © 2010 American Institute of Physics. [doi:10.1063/1.3451465]

Graphene is an emerging material of atomic-scale devices on account of its outstanding physical properties.¹ Recently, one of the focused applications of graphene is a semiconductor device such as a field emission transistor.^{2–4} Since pristine graphene is a zero-gap semiconductor, it is essential for the application that an energy gap is opened between the conduction and valence bands around a Dirac energy. A variety of techniques have been developed to open the energy gap. A representative technique in monolayer (ML) graphene is to use a form of a nanoribbon resulting in a quantum confinement effect.⁵ Typical techniques in bilayer graphene are to control the carrier density and external electric field.^{2,3} The carrier density was controlled to cause a finite interlayer energy difference between the two graphene layers of bilayer graphene.⁶ An external electric field was applied along the perpendicular direction to the graphene layers to induce asymmetry between the two graphene layers, where there are also carrier density changes in the two graphene layers in a device.⁷ For this reason, the carrier density in a device based on bilayer graphene is one of dominant factors. The band engineering of bilayer graphene was first reported for K-adsorbed epitaxial bilayer graphene grown on a 6H-SiC(0001) surface by Ohta *et al.*⁶ The electronic band structure of the K-adsorbed bilayer graphene was explained in terms of the tight-binding model. However, the continuous change in the electronic band structure as a function of K coverage has not been reproduced using first-principles calculations. This might be because the size of the unit cell should be changed as a function of K coverage and a large unit cell is needed at low K coverage. Another difficulty in the calculations is that K-adsorbed bilayer graphene does not form a well-defined superstructure, even though most metal atoms prefer the hollow site of the graphene layer.

In this study, the distances between bilayer graphene and metal atoms were adjusted instead of changing the unit cell

size of metal-adsorbed bilayer graphene as a function of metal coverage, as shown in Fig. 1(a).⁸ This allows first-principles calculations to reproduce the continuous changes in the electronic band structure of metal-adsorbed bilayer graphene as a function of metal coverage. Another advantage of the first-principles calculations is that the orbital characteristics of a metal or molecule can be taken into account, which is in contrast to the tight-binding model and the use of background charge.

VASP package was used for the first-principles calculations based on density functional theory.⁹ The potentials of the electron–ion interactions and the exchange and correlation parts of the electron–electron interactions were described by the projected augmented wave¹⁰ and generalized gradient approximation,¹¹ respectively. The plane waves were used to describe the electron wave functions, where the kinetic energies of electrons were below 400 eV. A 3×3 Monkhorst–Pack \vec{k} -point mesh on the surface Brillouin zone was used to calculate the total energy.¹² The shift in the Fermi energy away from the Dirac point of undoped free standing bilayer graphene is E_D , the energy gap at the K point is E_g^K , and the energy gap at the vicinity of the K point is E_g , as shown in Fig. 1(f).¹³ We note that the E_g^K and E_g are local energy gaps rather than the energy gaps of whole electronic band structures.

Figure 1 shows the change in the electronic band structure of bilayer graphene as a function of the distance between the Na atoms and upper graphene layer R_1 . A-B stacked bilayer graphene was chosen because the epitaxial bilayer graphene on a 6H-SiC(0001) surface has A-B stacking.⁶ Most metal atoms prefer energetically the hollow sites of a graphene layer and the 2×2 superstructures at metal coverage of 1/4 ML.^{14,15} For this reason, a 2×2 superstructure with Na coverage of 1/4 ML was used. The Na atoms were located at the hollow sites, as shown in Fig. 1(a). Only R_1 was changed while maintaining the 2×2 superstructure and Na coverage to control a charge transfer from the Na atoms to bilayer graphene. Figure 1(b) shows the electronic band

^{a)}Electronic mail: ohdh@skku.edu.

^{b)}Electronic mail: jrahn@skku.edu.

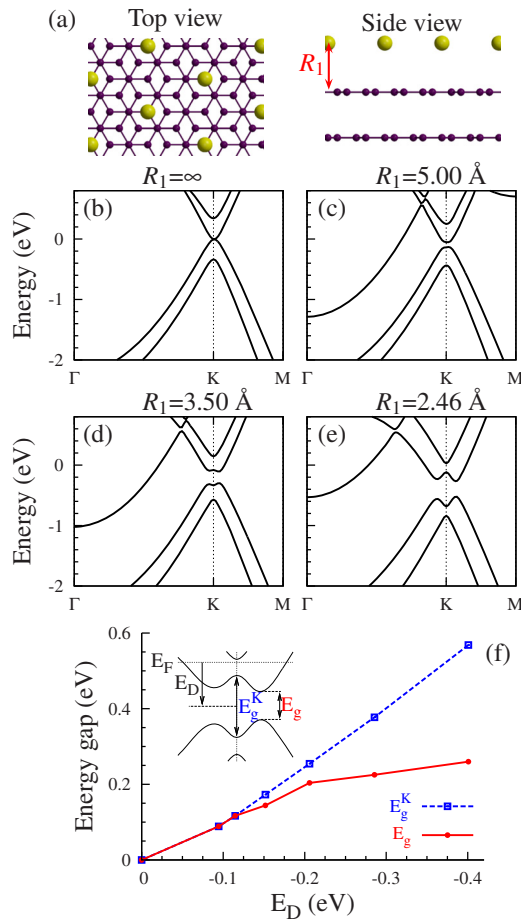


FIG. 1. (Color online) (a) The top and side views of the atomic structure of Na-adsorbed bilayer graphene, where R_1 is the distance between the Na atoms and upper graphene layer. The electronic band structures of (b) the pristine bilayer graphene and [(c)–(e)] Na-adsorbed bilayer graphene. (f) Changes in E_g and E_g^K as a function of a E_D , where the schematic diagram of the electronic band structure of the bilayer graphene is in the inset.

structure of undoped bilayer graphene, where an E_D is located at the Fermi energy. When Na atoms were attached to the upper graphene layer, the E_D moved downward and consequently the E_g became larger, as shown in Fig. 1(c). As Na atoms were closer to the upper graphene layer, the E_g became larger and the E_D shifted to a higher binding energy [see Figs. 1(d) and 1(e)]. The E_D change suggests that the dependence of the electronic band structure of bilayer graphene on metal or molecular coverage in an experiment can be reproduced by controlling R_1 in the first-principles calculations because a metal or molecule does not induce any significant structural deformation of bilayer graphene.^{14,15} Figure 1(f) shows that the changes in the E_g and E_g^K are different. This is because, in the tight-binding model, E_g and E_g^K are approximately proportional to $|U|\gamma/\sqrt{\gamma^2+U^2}$ and U , respectively, where U is the interlayer energy difference and γ is the interlayer tunneling amplitude.^{13,16}

The representative experiment for the band engineering of bilayer graphene using metal atoms is angle-resolved photoemission spectroscopy measurement of Ohta *et al.*⁶ In the experiment, K atoms were adsorbed on bilayer graphene grown on a 6H-SiC(0001) surface, where the bilayer graphene with an E_g of approximately 130 meV is n-type because of electron transfer from the bulk SiC. With increasing K coverage, the E_g was reduced and then closed at opti-

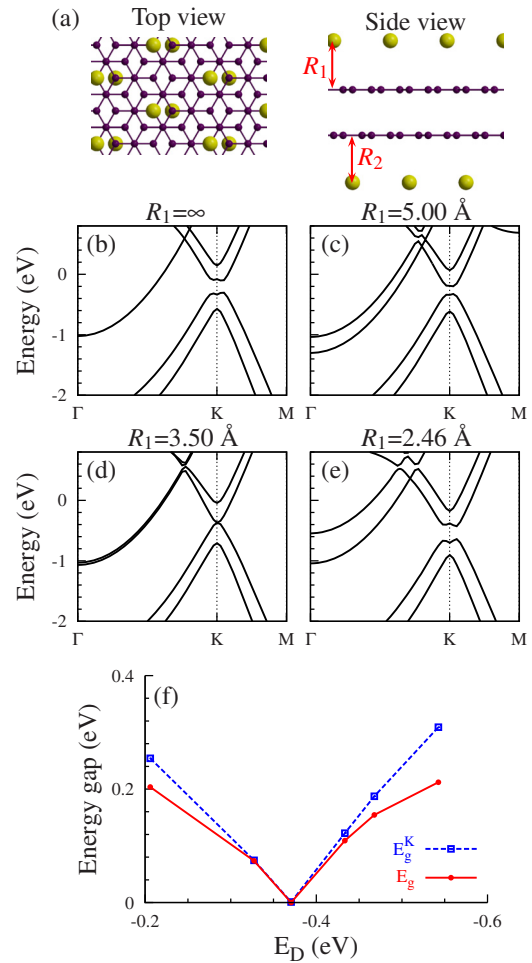


FIG. 2. (Color online) (a) The top and side views of the atomic structure of Na-adsorbed n-type bilayer graphene, where R_1 (R_2) is the distance between the Na atoms and upper (lower) graphene layer. The electronic band structures of (b) the n-type bilayer graphene and [(c)–(e)] Na-adsorbed n-type bilayer graphene. (f) Changes in E_g and E_g^K as a function of a E_D .

mal K coverage. Above the optimal K coverage, the E_g began to open again and became larger at higher K coverage. The distance-controlled theoretical calculations were applied to the metal-adsorbed n-type bilayer graphene to examine its validity. First, Na atoms were attached under the lower graphene layer to reproduce the electronic band structure of n-type bilayer graphene, as shown in Fig. 2(a). The distance between the Na atoms and lower graphene layer R_2 to produce an E_D of 206 meV was 3.5 Å [see Fig. 2(b)]. Second, additional Na atoms were attached to the upper graphene layer and R_1 was controlled, as performed on the undoped bilayer graphene. As the additional Na atoms approached the upper graphene layer, the E_D moved downward, as shown in Figs. 2(b)–2(d). On the other hand, the E_g was reduced at $R_1 > R_2$ and closed at $R_1 = R_2$. At $R_1 < R_2$, the E_g opened again and became larger, as shown in Figs. 2(b)–2(f). This supports that the distance-controlled theoretical calculations can reproduce the overall change in the electronic band structure of metal-adsorbed n-type bilayer graphene.

The distance-controlled theoretical calculations were also applied to p-type bilayer graphene. The difficulty in the band engineering of p-type bilayer graphene in an experiment is that the E_D and E_g cannot be measured accurately by angle-resolved and invert photoemission spectroscopy. The change in the electronic band structure of the p-type bilayer

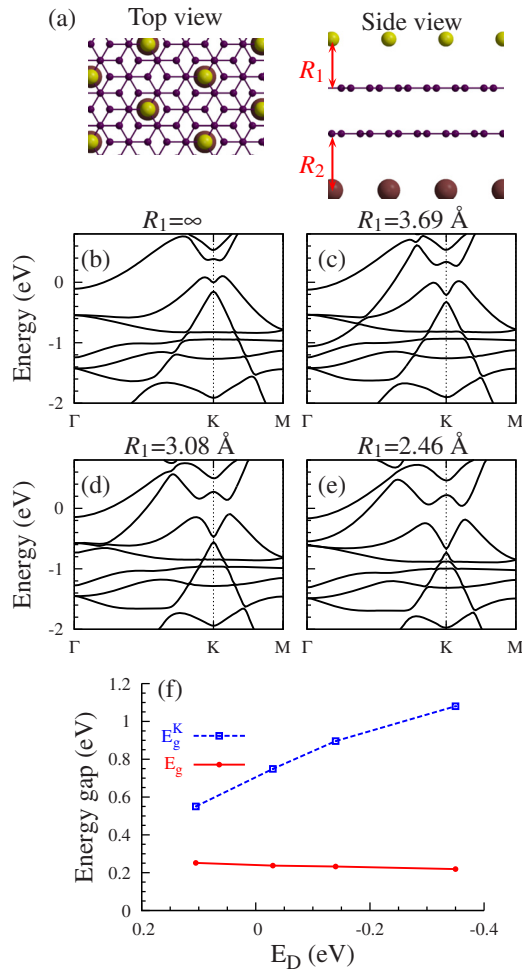


FIG. 3. (Color online) (a) The top and side views of the atomic structure of Na-adsorbed p-type bilayer graphene, where R_1 (R_2) is the distance between the Na (Pt) atoms and upper (lower) graphene layer, respectively. The electronic band structures of (b) the p-type bilayer graphene and [(c)–(e)] Na-adsorbed p-type bilayer graphene. (f) Changes in E_g and E_g^K as a function of a E_D .

graphene as a function of metal coverage was predicted using the distance-controlled theoretical calculations. p-type bilayer graphene was prepared by attaching Pt atoms under the lower graphene layer, as shown in Fig. 3(a).⁸ The p-type graphene has an E_g of 252 meV and a E_D of 105 meV [see Fig. 3(b)]. As performed on the n-type bilayer graphene, Na atoms were attached to the upper graphene layer. The E_D shifted downward and the E_g^K became larger as reducing R_1 [see Figs. 3(c)–3(e)], as observed on the n-type bilayer graphene. Compared to the n-type bilayer graphene, the E_g was almost independent of R_1 , as shown in Fig. 3(f). These results suggest how to control the electronic band structure of bilayer graphene by electron and hole donors. One of electron and hole donors should be adsorbed on an undoped

bilayer graphene to control an E_g efficiently. Electron (hole) donors should be adsorbed on p-type (n-type) bilayer graphene to control the E_D of bilayer graphene with a robust E_g . On the other hand, the E_g and E_g^K in Figs. 1–3 are optical gaps, while the whole electronic band structures are metallic without an energy gap. Hence the E_g and E_g^K can be measured by an optical experiment rather than a transport experiment.

In conclusion, band-engineered bilayer graphene was studied using first-principles calculations. The continuous changes in the electronic band structures of undoped, n-type, and p-type bilayer graphene were calculated as a function of metal coverage by controlling the distance between the metal atoms and bilayer graphene while maintaining the adsorption site and superstructure. The theoretical method is valid because the electronic band structure of bilayer graphene is dominated by the distribution of the carrier density within bilayer graphene. The theoretical method is more useful when metal atoms or molecules do not form a superstructure on bilayer graphene or the E_D is above the Fermi energy in an experiment.

This study was supported by the Korea Science and Engineering Foundation (KOSEF) grant funded by the Korea government (MEST) (Grant No. 2009-0080512) and Priority Research Centers Program through the National Research Foundation of Korea (NRF) (Grant No. 20090094026) and the Converging Research Center Program (Grant No. 2009-0081966).

- ¹K. S. Novoselov, A. K. Geim, S. V. Morozov, D. Jiang, Y. Zhang, S. V. Dubonos, I. V. Grigorieva, and A. A. Firsov, *Science* **306**, 666 (2004).
- ²J. B. Oostinga, H. B. Heersche, X. Liu, A. F. Morpurgo, and L. M. K. Vandersypen, *Nature Mater.* **7**, 151 (2008).
- ³Y. Zhang, T.-T. Tang, C. Girit, Z. Hao, M. C. Martin, A. Zettl, M. F. Crommie, Y. R. Shen, and F. Wang, *Nature (London)* **459**, 820 (2009).
- ⁴M. F. Craciun, S. Russo, M. Yamamoto, J. B. Oostinga, A. F. Morpurgo, and S. Tarucha, *Nat. Nanotechnol.* **4**, 383 (2009).
- ⁵M. Y. Han, B. Özyilmaz, Y. Zhang, and P. Kim, *Phys. Rev. Lett.* **98**, 206805 (2007).
- ⁶T. Ohta, A. Bostwick, T. Seyller, K. Horn, and E. Rotenberg, *Science* **313**, 951 (2006).
- ⁷P. Gava, M. Lazzari, A. M. Saitta, and F. Mauri, *Phys. Rev. B* **79**, 165431 (2009).
- ⁸G. Giovannetti, P. A. Khomaykov, G. Brocks, V. M. Karpan, J. van den Brink, and P. J. Kelly, *Phys. Rev. Lett.* **101**, 026803 (2008).
- ⁹G. Kresse and J. Furthmüller, *Comput. Mater. Sci.* **6**, 15 (1996).
- ¹⁰P. E. Blöchl, *Phys. Rev. B* **50**, 17953 (1994); G. Kresse and D. Joubert, *ibid.* **59**, 1758 (1999).
- ¹¹J. P. Perdew, K. Burke, and M. Ernzerhof, *Phys. Rev. Lett.* **77**, 3865 (1996); **78**, 1396 (1997).
- ¹²H. J. Monkhorst and J. D. Pack, *Phys. Rev. B* **13**, 5188 (1976).
- ¹³E. McCann, *Phys. Rev. B* **74**, 161403 (2006).
- ¹⁴S.-M. Choi and S.-H. Jhi, *Appl. Phys. Lett.* **94**, 153108 (2009).
- ¹⁵K. T. Chan, J. B. Neaton, and M. L. Cohen, *Phys. Rev. B* **77**, 235430 (2008).
- ¹⁶Y. Guo, W. Guo, and C. Chen, *Appl. Phys. Lett.* **92**, 243101 (2008).